Environmental Science & Technology

pubs.acs.org/est

Article

Adsorption of PFAAs in the Vadose Zone and Implications for Long-Term Groundwater Contamination

William R. Gnesda,* Elliot F. Draxler, James Tinjum, and Christopher Zahasky

Cite This: *Environ. Sci. Technol.* 2022, 56, 16748−16758

Read Online

ACCESS | Metrics & More | Article Recommendations | Supporting Information

ABSTRACT: Perfluoroalkyl acids (PFAAs) are persistent environmental contaminants that sorb to air−water and solid interfaces throughout the vadose zone. These sorption processes lead to decadal leaching of PFAS from the source zones to groundwater systems. While these processes are increasingly well understood, critical gaps exist in describing the vertically variable adsorption in the presence of vadose zone heterogeneity and methods for efficiently upscaling the laboratory observations to predict field-scale PFAA transport and retardation. In this work, we build upon fundamental theories and scalable relationships to define a semi-analytical framework for synthesizing and upscaling PFAA adsorption in heterogeneous vadose zone systems. Solid-phase and air−water interfacial adsorption are quantified mechanistically for several PFAAs and then applied to a contaminated site in Northern Wisconsin. The results highlight the dominance of air−water and organic carbon solid-phase adsorption processes in the vadose zone. Strong sorption heterogeneity—driven by depth-dependent adsorption mechanisms—produces complex spatially variable retardation profiles. We develop vadose zone retardation potentials to quantify this field-scale heterogeneity and propose vertical integration methods to upscale spatially resolved information for transport modeling. This work highlights the importance of accounting for multiscale and multiprocess heterogeneity for accurately describing and predicting the long-term fate and transport of PFAAs in the subsurface.

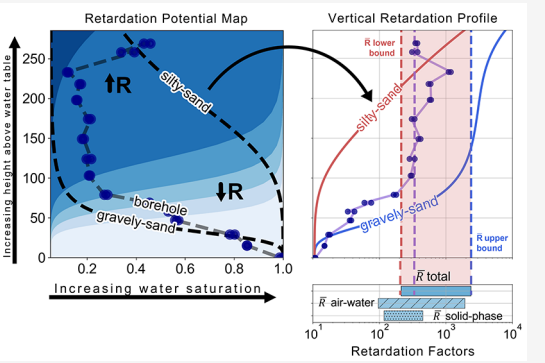

KEYWORDS: *PFAS, PFAAs, vadose zone, heterogeneity, contaminant transport*

INTRODUCTION

Per- and poly-fluoroalkyl substances (PFAS) are a broad group of synthetic contaminants comprising thousands of individual species that have been shown to be toxic to humans and ecosystems.[1] Perfluoroalkyl acids (PFAAs) are a specific subgroup of PFAS that contribute to widespread environmental contamination through their use in aqueous firefighting foams (AFFF),[2] leakage of landfill leachate,[3] agricultural application of PFAA-contaminated biosolids,[4] and PFAA production facilities.[1] Numerous field investigations have highlighted PFAA concentrations in excess of the EPA lifetime health advisory limits decades after the most recent applications. This observed long-term leaching phenomenon combined with historic environmental loading has presented alarming implications for transport between the unsaturated zone and groundwater.[5−8]

Many anionic PFAAs of concern possess surface-active properties, including a tendency to adsorb to fluid−fluid and fluid−solid interfaces.[9,10] The physicochemical properties of PFAAs driving this behavior are the result of the headgroup containing an organic functional group, such as a carboxylic or sulfonic acid, and the fluorinated tail. The hydrogen atom associated with the functional group readily dissolves in water creating a negatively charged, hydrophilic headgroup. The negatively charged headgroup of anionic PFAAs may also drive electrostatic attraction to the interfaces of solid substrates. In contrast, the tail end of the PFAA molecule is both hydrophobic and lipophobic due to the strong electronegativity of carbon−fluorine bonds.[11] PFAAs also exist in cationic and zwitterionic forms, which have demonstrated a strong sorption behavior to soils.[10,12−14]

A number of mechanisms control the timing of PFAA transport from surface sources to groundwater systems. PFAAs sorb to the solid surfaces of soils and sediments, with the extent of sorption influenced by properties such as pH,[15] total organic carbon (TOC),[16] mineral assemblages,[17,18] and anion exchange capacity (AEC).[19] PFAA adsorption at air−water interfaces is a function of the water chemistry, PFAA aqueous concentration, surface excess[20] and the air−water interfacial area.[21] Recently developed models have highlighted the extent to which air−water interfacial sorption processes dominate the

Received: June 7, 2022
Revised: October 31, 2022
Accepted: November 2, 2022
Published: November 17, 2022

timing of PFAS transport through the vadose zone in homogeneous media.[22,23]

Approximations of PFAA fate and transport in the subsurface require the quantification of solid-phase and air−water adsorption by experimental methods. To quantify solid-phase adsorption, batch-type and saturated column experiments are commonly performed and analyzed by liquid chromatography-mass spectrometry (LC-MS/MS).[19,24] Current approaches to measure PFAA air−water adsorption in unsaturated porous media consist of interfacial tension-based approaches,[20,25] unsaturated column retardation approaches,[26−29] and batch system mass balance approaches.[30] These approaches have demonstrated that adsorption is dependent upon the affinity of PFAA for organic carbon, mineral phases, and air−water interfaces; the affinity is further found to be a function of the PFAA carbon chain length, functional group, pH, and linear versus branched PFAA isomers.[16,17,29,31] After quantification, the adsorption mechanisms are typically uniformly applied to homogeneous unsaturated solute transport models.[22,23,32−34]

Quantifying the PFAA transport in realistic geologic systems requires approaches that can account for heterogeneous adsorption and preferential flow pathways that create a dynamic and complex contaminant transport behavior. To forecast contaminant migration under complex subsurface conditions, ensemble-based modeling approaches have been introduced to account for model and geologic uncertainty.[35−37] Implementation of ensemble-based transport modeling of PFAAs requires running a large number of models that represent the range of uncertainty and heterogeneity of hydrogeologic conditions and PFAA adsorption at a given contaminated site. The computational limits of running a large number of model realizations warrant the development of efficient theoretical and numerical approaches to upscale PFAA adsorption parameters from the laboratory to the field scale.

The objective of this study is to integrate the PFAA adsorption theory into a mechanistic framework for estimating PFAA retardation throughout heterogeneous unsaturated systems at the field scale. Interfacial tension-based approaches are used to quantify the air−water adsorption of PFAA species of different carbon chain lengths and functional groups in background electrolyte concentrations ranging from 0 to 0.1 molar [M] NaCl, simulating the conservative end members of rainwater and biosolid effluents, respectively. Soil sample properties and capillary pressure measurements from a field site adjacent to the impacted municipal wells in Northern Wisconsin are used to determine solid-phase adsorption and quantify the extent of capillary heterogeneity corresponding to soil−water saturation. The existing models for describing PFAA adsorption to air−water interfaces and solid phases are expanded to describe adsorption as a function of water saturation and height above the water table under hydrostatic conditions. Using routine site-specific measurements, we demonstrate a semi-analytical approach for estimating depth-dependent PFAA retardation in geologically heterogeneous systems and techniques to simplify vertically variable adsorption profiles in the vadose zone for efficient implementation into risk-based modeling schemes.

MATERIALS AND METHODS

PFAA Transport Model. The retardation factor, R, describes the degree to which a solute reacts with phase boundaries within porous media. With the application of an appropriate advection−dispersion−reaction equation, the retardation factor can be used to estimate the speed of a reactive solute relative to a nonreactive tracer. PFAAs in the aqueous phase undergo equilibrium adsorption between the solid-phase and air−water interfaces according to the equation[10,22,23,32,38,39]

$$R = 1 + \frac{K_d \rho_b}{\phi S_w} + \frac{K_{aw} A_{wi}}{\phi S_w} \quad (1)$$

Here, the volumetric water content is given in terms of water saturation (S_w) and porosity (ϕ). The solid-phase adsorption of PFAA is expressed by the soil−water distribution coefficient (K_d) and the bulk density of the soil (ρ_b). The value of K_d is determined by the sorption potential of both organic carbon and mineral phases present in the soil. The fraction of organic carbon contained within soil has been shown to drive PFAA adsorption onto the solid phase.[16,18,19]

The retardation of PFAAs due to air−water adsorption within the vadose zone is represented by the air−water adsorption coefficient (K_{aw}) and the air−water interfacial area (A_{wi}) approximated by relationships between surface tension and the aqueous concentration in contact with the air−water interface.[10,39,40] At some contaminated vadose zone sites, several other forms of multiphase retardation may occur for PFAAs, including air−water partitioning, nonaqueous phase liquid (NAPL)−water partitioning, and NAPL−air partitioning.[22] However, co-contamination of PFAAs and NAPL has not been reported at the field site in this study, and the magnitudes of air−water and solid-phase adsorption are known to be the dominant mechanisms, so other forms of retardation are neglected.[26]

Solid-Phase Adsorption. The soil−water adsorption coefficient, K_d, was determined from batch-type experiments and literature relationships. Batch methods were developed from previous solid-phase sorption experiments[16,19] and analyzed by LC-MS/MS.[41] Briefly, PFAAs with aqueous concentrations ranging from 0.4 to 270 parts per billion (ppb) in deionized water and 0.1 M NaCl solution were placed in contact with the sediment samples and agitated at either 24 or 48 h. After agitation, an aliquot of the liquid was preserved and analyzed by LC-MS/MS to determine the concentration of PFAAs remaining in the aqueous phase—no pH adjustments were applied. Soil-to-solution ratios and adsorption equilibrium experiments were conducted prior to isotherm quantification, resulting in the selection of appropriate ratios and conservative contact times of 24 and 48 h.[42] Experiments were performed with blanks to monitor sorption to containers and instrument contamination. A full description of the methods and analysis is provided in the Batch methods and isotherms section of Supporting Information (SI).

Air−Water Interfacial Adsorption. Adsorption at air−water interfaces was determined using Freundlich and Langmuir adsorption models with an interfacial tension-based approach.[20,25] Briefly, the surface tension of individual PFAA species was measured in ultrapure water and 0.1 M NaCl solution. The Langmuir−Syszkowski[20,44] and Freundlich[43,45] adsorption equations were then employed to determine the surface excess and adsorption coefficients at the air−water interface. Approximations of A_{wi} were derived from literature relationships described in more detail below.[46,47]

https://doi.org/10.1021/acs.est.2c03962
Environ. Sci. Technol. 2022, 56, 16748−16758

Assuming an ideal behavior of aqueous-phase solutions, the Gibbs adsorption equation may be employed to describe the molar mass of PFAAs sorbed at air−water interfaces.[20,25,43] The Gibbs adsorption equation is

$$\Gamma = \frac{-1}{\mathcal{R}T}\frac{\partial\sigma}{\partial \ln(C^*)} \quad (2)$$

Here $\mathcal{R}$ is the gas constant [mJ mol^{-1} K^{-1}], T is the temperature at the time of the measurements [K], and σ is the surface tension [mN m^{-1}]. The mean ionic activity, C^*, is the surface activity-corrected concentration of PFAAs in the presence of background counter-ions.

For ionic surfactant solutions containing any background counter-ions, the measured surface tension of the solution will be lower than its pure-water counterpart.[20,25,43,48,49] These deviations from ideal surface behavior are difficult to extrapolate for increasingly dilute PFAA solutions without correcting for background electrolyte compositions.[49] Therefore, the correction, C^*, for PFAAs dissolved in solution must be applied to appropriately represent the surface activity behavior of PFAAs as given in eq 3[48]

$$C^* = \sqrt{\gamma^2 \cdot C(C + C_{salt})} \quad (3)$$

Here, the mean ionic activity is calculated from the averaged activity coefficient (γ), the surfactant concentration (C), and the concentration of salt (C_{salt}) in solution. The activity coefficient is calculated from a form of the Debye−Huckel Equation.[50,51] The mean ionic activity correction attempts to describe the surface activity of ionic PFAAs corrected for the background counter-ion influence on the overall surface tension of the solution.[49]

Surface excess, or the quantity of PFAAs adsorbed per area of the air−water interface, is calculated by fitting the surface tension measurements at various aqueous concentrations to an appropriate adsorption model. For comparative purposes, the Freundlich (eq 4) and Langmuir−Syszkowski (eq 5) adsorption models were selected to describe PFAA adsorption at the air−water interface for solutions below the critical micelle concentration (CMC).[20,43]

$$\Gamma = K_f(C)^N \quad (4)$$

$$\Gamma = \frac{\Gamma_{max}\beta C}{1 + \beta C} \quad (5)$$

In eq 4, Γ is the surface excess [mol m^{-2}], and K_f and N are the fitting parameters. For eq 5, Γ_{max} and β are fitting parameters representing the interfacial sorption capacity [mol m^{-2}] and adsorption affinity coefficient [m^3 mol^{-1}]. If the species exists as a salt form or contains any background counter-ions, then C is converted to C^* using eq 3, assuming complete dissociation of PFAAs and counter-ions occurs.

Respectively integrating eqs 4 and 5 into eq 2 results in an approximate description of the surface tension in terms of the Freundlich and Langmuir−Syszkowski adsorption models.[43]

$$\sigma = \sigma_0 - \mathcal{R}TK_f\frac{(C)^N}{N} \quad (6)$$

$$\sigma = \sigma_0 - \mathcal{R}T\Gamma_{max}\ln(1 + \beta C) \quad (7)$$

Here, σ_0 is the surface tension of the solution without PFAS. The parameters K_f, N, Γ_{max}, and β are all determined from fits to surface tension measurements at various molar concentrations. The model was fit with a nonlinear generalized reduced gradient method to minimize the sum of squared residuals. A detailed description of the experimental surface tension methods, along with isotherm coefficients, is provided in the SI.

The surface excess relates the aqueous-phase solute concentration to the air−water adsorption coefficient, K_{aw} [M], following the equation

$$K_{aw} = \frac{\Gamma}{C} \quad (8)$$

The air−water adsorption coefficient can be influenced by physicochemical properties like the chain length[52] and the presence of co-occurring PFAS.[43,53,54] In field settings, PFAS are likely to occur as multi-component mixtures with several precursory and terminal products.[55,56] The value of K_{aw} and Γ are also influenced by solution properties, namely, ionic strength, pH, and temperature.[10,57] It is important to note that different adsorption models can produce disparate predictions of K_{aw} at end-member concentration ranges.[43,58] Therefore, the application of an adsorption model must appropriately consider the concentration range and environmental conditions of interest.

The solid-phase and air−water adsorption behaviors of four PFAAs were examined for this study. Each of the four PFAAs—PFHxS, PFOA, PFOS, and PFDA—shows a range of increasing hydrophobic carbon chain lengths (Table S1 in SI) and functional groups and are representative of the typical legacy PFAS found at contaminated sites.[59]

Air−Water Interfacial Area. Applying the PFAA-specific physicochemical properties contained within K_{aw} to the vadose zone requires the determination of the saturation-dependent air−water interfacial area of the porous medium. The air−water interfacial area of several soils and sediments has been quantified by empirical equations relating the van Genuchten model for capillary pressure characteristic curves, the sediment-specific surface area, grain-size distribution, and monolayer saturation.[46,47] The van Genuchten equation[60] is used to construct an approximate water saturation (S_w) profile using eq 9.

$$S_w = S_r + (1 - S_r)((1 + \alpha_v P_c)^{n_v})^{-(1-(1/n_v))} \quad (9)$$

Here, S_r is the residual water saturation [-] and P_c is the capillary pressure [kPa]. The terms α_v and n_v are constants fit to the measured capillary pressure data and represent the inverse of entry pressure [1/kPa] and the pore-size distribution [-], respectively.[60] Converting P_c to an elevation above the water table scales the capillary pressure−water saturation function to physically representative unsaturated systems.

For a given S_w profile determined from eq 9, the air−water interfacial area can then be calculated by the following relationship.[46]

$$A_{wi} = s[1 + (\alpha_{wi}(S_w - S_m))^{n_{wi}}]^{-m} \quad (10)$$

Here, A_{wi} is the air−water interfacial area [cm^{-1}], s is the normalized specific surface area, and S_m is the monolayer saturation. The terms α_{wi}, n_{wi}, and m are coefficients correlating to the uniformity coefficient of the porous medium. For a given uniformity coefficient, $\alpha_{wi} = 14.3\cdot\ln(U) + 3.72$. For uniformity coefficients greater than or equal to 3.5, $m = 1.2$ and $n_{wi} = \frac{1}{2-m}$.[46,47]

https://doi.org/10.1021/acs.est.2c03962
Environ. Sci. Technol. 2022, 56, 16748−16758

The Brunauer−Emmett−Teller (BET) theory is commonly employed to quantify s, as well as the pore-size distribution and pore volume by nitrogen gas physisorption.[61] The normalized specific surface area of soil samples was determined for air-dried soil samples using nitrogen BET and the bulk density [g cm^{-3}] of the soil using a Quantachrome NovaTouch LX BET surface characteristic analyzer. Monolayer saturation was neglected in this study.

Vertical Integration Framework. With air−water and solid-phase adsorptions quantified as functions of the height above the water table, the breakthrough time for a source of PFAAs to reach the water table can be estimated by vertically integrating[62] the retardation profile with depth using the following equation.

$$\bar{R} = \frac{1}{H}\int_0^H R(z)\mathrm{d}z \tag{11}$$

Here, $\bar{R}$ is the depth-averaged retardation and H is the height of the vadose zone. The integral is taken from the base of the vadose zone to the surface. This depth-averaged approach synthesizes complex vadose zone retardation profiles into single values for implementation into computationally efficient one-dimensional (1D) unsaturated transport models.

Oneida-Rhinelander Airport Geologic Setting and Soil Properties. Site characterization of the geology and vadose zone conditions at Oneida-Rhinelander Airport (ORA) provides a case study to demonstrate and apply the proposed PFAA transport and retardation framework. Several PFAAs of concern have been identified in concentrations exceeding 70 ng L^{-1}, resulting in the shutdown of two municipal groundwater drinking wells pumping from the unconfined groundwater aquifer adjacent to the airport.[63] The extent of contamination and source zones are under active investigation.

Located in the Northern Highlands geologic region of Wisconsin, the subsurface around ORA is dominated by stratified sand and gravelly sand glacial melt-water deposits with pockets of organic-rich peaty soils throughout.[64,65] Soil samples from three boreholes, designated B004, B005, and B006, were collected near the two municipal wells just outside the southern airport boundary to measure steady-state water content. The boreholes were selected because of the close proximity to the two municipal drinking wells and were easily accessible. To describe the vadose zone water saturation profile, in situ and lab-measured capillary pressure characteristic curves were constructed for the study site following the van Genuchten model (eq 9). Additional grain-size distribution and loss on ignition (LOI) analyses were performed to determine the uniformity coefficients and organic carbon content. Details of the sediment characterization and capillary pressure curve construction are provided in the SI.

RESULTS

Solid-Phase Adsorption Coefficients. The development of theoretical or empirical estimations of PFAA solid-phase adsorption is key for reducing sample costs and mitigating the challenges associated with PFAS analyses. There exists significant scatter in the reported range of K_d for several PFAAs attributed to the variability in soil pH, clay content, and organic carbon content.[15] The organic carbon partitioning coefficient, K_{oc}, has been shown to under-represent PFAA solid-phase sorption,[15,16,18] but as the carbon chain length increases, the influence of organic carbon-associated solid-phase adsorption increases.[18] Depth analysis of grain-size distribution and LOI shows that the content of fines (middle panel of Figure 1) and organic carbon (right panel of Figure 1) decreases with depth in the vadose zone.

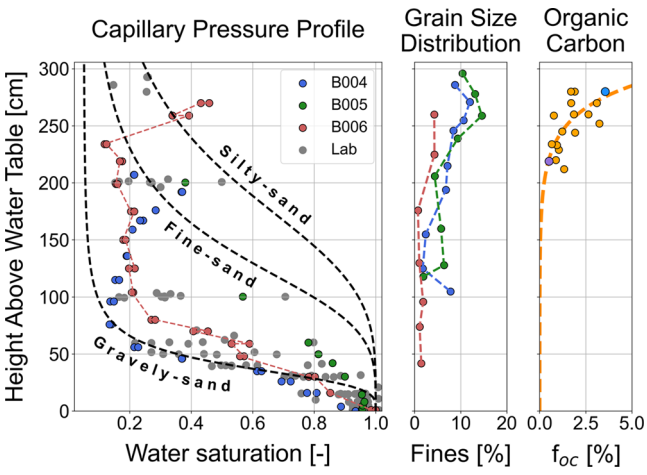

Figure 1. (Left) The water saturation of boreholes (B004, B005, B006) and homogenized soil samples (Lab) were found at several locations throughout the ORA field site. ORA is primarily composed of glacial outwash sediments, coarsening with depth. The dashed black lines correspond to capillary pressure curve fits to the measured data, while the red dashed line traces the in situ curve of B006. (Middle) The fines distribution corroborates the findings from the field capillary pressure curves, where finer material can be found in the upper section. (Right) The distribution of organic carbon as a function of depth fit with an appropriate function. Blue and purple points correspond to the organic carbon content of solid-phase adsorption samples. This figure highlights the vertical heterogeneity of properties impacting PFAA adsorption at the ORA field site.

Batch-type experiments were used to derive the K_d for individual PFAAs in contact with low-organic-carbon-content ORA soils. Soil samples collected at a depth of 140−190 cm from ORA had minimal organic carbon content (<0.1%) and were found to have negligible amounts of PFHxS, PFOA, and PFDA. Sorption for PFOS in these lower soil profiles was best described by a linear isotherm in DI water and 0.1 M background NaCl solution. The determined linear K_d values for PFOS attachment to ORA soils was 0.1 and 0.34 L kg^{-1} for solution compositions of DI and 0.1 M NaCl, respectively. Batch measurements and analysis of fired and air-dried soil samples showed similar adsorption behaviors, further indicating that K_d is representative of mineral-phase adsorption processes and not adsorption to organic carbon in the lower soil profile.

In addition to the batch experiments in the low-organic-carbon soils, one high-TOC (3.55%) surficial sediment was analyzed to compare the significance of organic carbon sorption at the field site. This sample was taken from a mixture of soils collected from the surface to 30 cm depth. All PFAA species displayed sorption to this soil sample, but analytical losses restricted the determination of an appropriate K_d for PFHxS, PFOA, and PFDA. The determined K_d for PFOS was 1.66 L kg^{-1}.

Based on these results, solid-phase adsorption of PFAAs onto ORA soils was calculated using the relationship $K_d = K_{oc}f_{oc}$—based on the available literature values of K_{oc}. $\log K_{oc}$ values were averaged across the reported range for the studied PFAAs, producing values for PFHxS, PFOA, PFOS, and PFDA

https://doi.org/10.1021/acs.est.2c03962
Environ. Sci. Technol. 2022, 56, 16748−16758

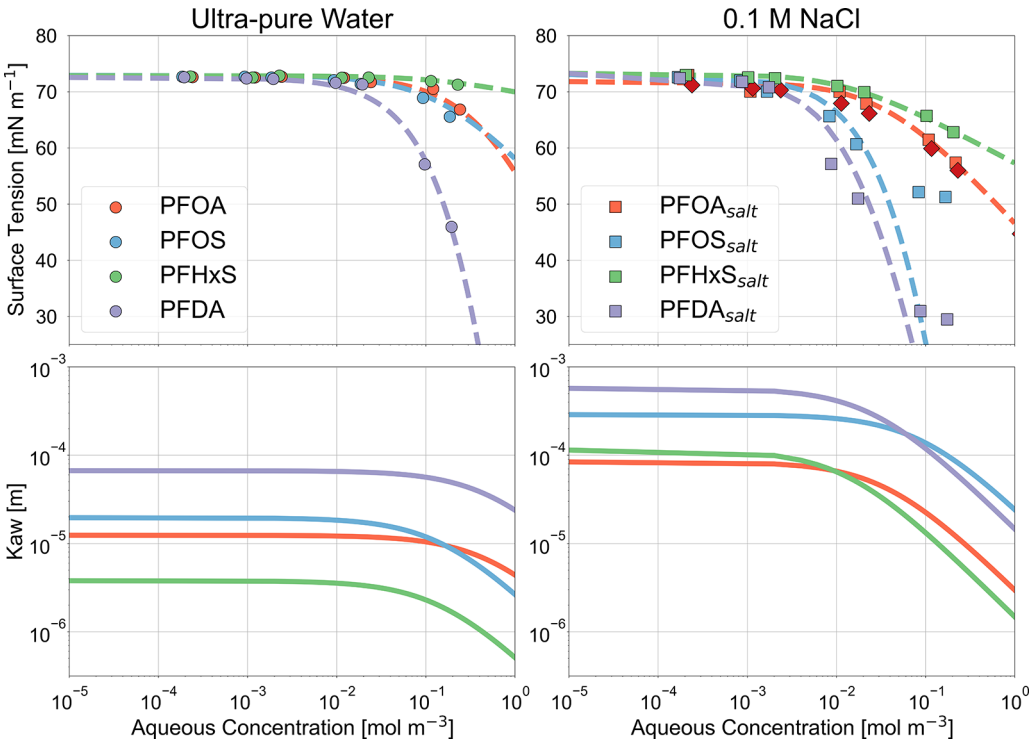

Figure 2. Surface tension and K_{aw} in ultrapure water and 0.1 M NaCl solution plotted against molar concentration. Dashed lines represent Langmuir−Syszkowski best fits. Fitting parameters are present in Table S2. Note, because the CMC boundary was heavily influenced by the addition of 0.1 M NaCl, fits were performed for concentrations of 10 mg L^{-1} and under. Additionally, PFOA measurements in saline solution were compared with previously measured data (diamonds).[27] Air−water adsorption coefficients are shown to be higher in saline conditions.

of 2.71, 2.62, 3.41, and 3.65, respectively.[11] log K_{oc} values have been shown as reasonable PFAA sorption approximations.[15,16] However, depending on the geologic material present, sorption of PFAA may be influenced by the ionic strength and pH of the solution. For example, the presence of monovalent and divalent cations in crushed limestones[66] and changes in sorbent surface charge due to pH conditions.[15] The organic carbon content relationship was used as a representative solid-phase adsorption approximation because the ORA field site is composed of quartz-rich sands at stable pH conditions. The measured distribution of organic carbon throughout the vadose zone was fit with an exponential function describing the change in organic carbon with depth (right panel of Figure 1) and paired to the log K_{oc} value of each PFAA. However, the measured K_d for the shallow soil sample is an order of magnitude lower than that determined from the K_{oc} relationship (89.96 L kg^{-1}), likely due to outliers in the literature data.

Air−Water Adsorption Coefficients. Surface tension measurements were used to relate aqueous PFAA concentrations to K_{aw}. Surface tension data for select PFAAs are presented in Figure 2—individual isotherm parameters can be found in the SI. For PFAAs in ultrapure water, both Freundlich and Langmuir−Syszkowski adsorption isotherms approximate the surface tension over environmentally relevant concentration ranges (0.01−10 parts per billion) of the well. The range of concentrations examined (0.1−100 mg L^{-1}) were all well below the CMC for an ultrapure solution, as indicated by a continuous decrease in surface tension across the measured range.[67] In the Langmuir−Syszkowski adsorption model, PFAAs with similar carbon chain lengths (PFOA and PFOS) display similar magnitudes of Γ_{max}, describing the maximum sorption capacity at the air−water interface. Similarities between β and the functional group are supported by previous observations.[68] The values of K_{aw} at dilute concentrations tend to increase with the number of carbon chains (Figure 2). These results highlight that chain length exerts a strong influence on air−water interfacial adsorption behavior.

PFAAs in high saline solution displayed significant decreases in both surface tension and the CMC boundary relative to PFAAs in ultrapure water, an observation supported by previous studies.[43,69] With the addition of 0.1 M NaCl, Γ_{max} increases, indicating that the presence of background salts increases the maximum surface adsorption capacity and thus the maximum air−water interfacial adsorption of PFAA when compared to ultrapure water solutions.

Capillary Pressure−Retardation Relationship. The capillary pressure characteristics of the sampled boreholes were determined to constrain the range of subsurface heterogeneity across the ORA field site and to construct A_{wi} profiles for different soil types. Equation 9 was fit across the measured range of lab and field capillary pressure data producing fits to the parameters α_v and n_v of 0.25 [kPa^{-1}] and 4.0 [-], respectively. This curve is illustrated by the gravelly sand dashed line in Figure 1. The residual water saturation (S_r) was measured to be between 0.049 and 0.057 from repeated laboratory measurements of the characteristic curves. Two additional capillary pressure curves are constructed to constrain the finer-grained components of the sediment. Capillary pressure curves representing fine and silty sands are fit with α_v and n_v values of 0.08 [kPa^{-1}] and 4.0 [-], and 0.055 [kPa^{-1}] and 4.0 [-], respectively. The average measured porosity for ORA is 0.42. Grain-size distribution analyses on multiple soil samples produced uniformity coefficients $\left(\frac{d_{60}}{d_{10}}\right)$

https://doi.org/10.1021/acs.est.2c03962
Environ. Sci. Technol. 2022, 56, 16748−16758

between 2 and 12 with an average of 4.99. The specific surface area of ORA soil samples, determined from N(2)-BET, was 5 [cm^2 g^{-1}] for an average bulk density of 1.53 [g cm^3].

Capillary pressure characteristic curves are a reflection of the local pore-size distribution in a porous media that serves to link the properties of the subsurface to PFAA air−water adsorption coefficients and retardation (eq 1). Using the laboratory results combined with the air−water interfacial adsorption theory, Figure 3 illustrates the hydrostatic PFAA retardation as a function of height above the water table. Figure 3 assumes homogeneous capillary pressure characteristics and shows the relative influence of the air−water and solid-phase retardation processes on the combined retardation profile using eq 1. The air−water interfacial retardation is calculated using the Langmuir−Syszkowski adsorption model and eq 8, and eq 10 for the gravelly sand capillary pressure curve shown in Figure 1.

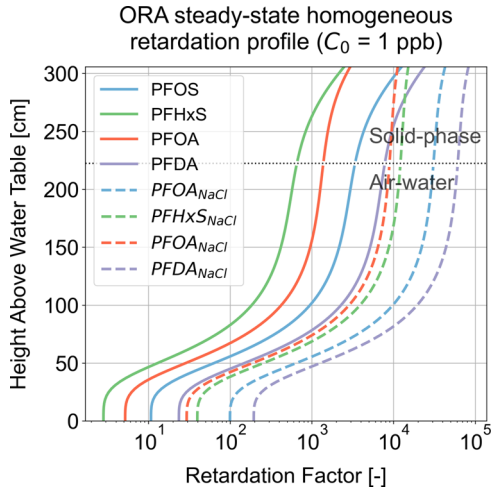

Figure 3. Air−water-associated retardation factor in relation to saturation and capillary pressure dependencies on A_{wi}. For PFAA in saline solution, retardation factors are magnified by approximately a factor of ten, as expected from the increases in the air−water adsorption coefficients measured in Figure 2. The dotted black line indicates the depth at which the dominant retardation process transitions from solid-phase to air−water adsorption. PFAAs with more carbon chains exhibit greater adsorption coefficients and thus stronger retardation profiles.

Air−water adsorption processes tend to dominate the retardation profile in the vadose zone with the additive effect of solid-phase sorption in the upper vadose zone, where the organic carbon content is high and water saturation is at a minimum, as shown in Figure 3. For the remaining profile, air−water interfacial adsorption is responsible for high retardation factors until the water saturation increases near the water table, reducing A_{wi} and thus R. PFAAs in both pure and saline solution display extreme retardation factors. A substantial increase is observed in the saline solutions, increasing the retardation factors by approximately 1 order of magnitude. At low water saturation conditions, these results suggest that PFAS is nearly immobile in the upper vadose zone where air−water and solid-phase adsorptions are the strongest.

Retardation in the Heterogeneous Vadose Zone. At field scales, PFAA transport is further complicated by the introduction of capillary heterogeneity across the vadose zone. Capillary heterogeneity describes the variation in capillary pressure characteristic behavior across different geologic porous media.[70,71] At the ORA site, capillary heterogeneity is driven by differences in the grain-size distributions of stratified glacial melt-water deposits that vary with depth. This heterogeneity can result in large fluctuations in steady-state water saturation as a function of depth—and thus fluctuations in air−water retardation—as illustrated near the top of boreholes B004 and B006 in Figure 1. The dashed lines in Figure 1 illustrate the range of measured capillary pressure profiles at ORA representing soils ranging in composition from gravelly sand to silty sand.

To accurately describe the PFAA retardation throughout a heterogeneous vadose zone, the range of saturation variability driven by capillary heterogeneity must be approximated. Capillary heterogeneity at a particular site, with consistent depositional and lithification processes, often exhibits a constant shape of the pore-size distributions such that the capillary entry pressure is scaled to describe the local variability in capillary pressure behavior.[72−74] In mathematical terms, this scaling is achieved by variations in the van Genuchten parameter α_v, the inverse of entry pressure. For fixed values of n_v, soils with a larger component of coarse material will exhibit higher values of α_v. Conversely, a greater content of fines will result in decreases in α_v.

To account for the full range of capillary characteristic curves at a given site—combined with depth-varying solid-phase sorption—Figure 4 maps the full range of possible PFAA retardation in the vadose zone. These vadose zone retardation potentials assume a constant pore-size distribution shape (n_v = 4.0), minimum residual saturation (S_r = 0.05), and average uniformity coefficient (U = 4.99), and utilize the air−water interfacial adsorption coefficients measured in ultrapure water for a concentration of 1 ppb for each PFAA species. Representative characteristic curves are plotted in Figure 4 to highlight the envelope of observed capillary heterogeneity based on the borehole and lab measurements illustrated in Figure 1. This approach enables the estimation of retardation at a given depth within the vadose zone and an associated water saturation—providing a first-order approximation of PFAA retardation throughout an entire contaminated site. The corresponding profiles for PFAA in 0.1 M NaCl solution are provided in the SI.

Site-Specific Vertically Integrated Retardation. The vertical integration framework provides a means to synthesize the impact of spatially heterogeneous adsorption properties on PFAA retardation at field sites. Figure 5 summarizes the adsorption diagrams presented in Figure 4 for PFOS in ultrapure water by showing the range of capillary pressure-constrained depth-averaged retardation factors accounting for site heterogeneity. Across a range of depths, air−water adsorption controls the maximum and minimum bounding retardation factors. The additive effect of both air−water and solid-phase processes creates a zone of high retardation in the upper vadose zone across the field site.

DISCUSSION

Solid-Phase Sorption Heterogeneity. The geologic media of ORA is primarily composed of quartz-rich sands with minimal Fe-oxides (Table S2), indicating that organic carbon is likely to drive sorption at the site.[15−17,66] Accounting for the variability of adsorption processes throughout the vadose zone is essential for accurate PFAA retardation estimation, the effect of which is highlighted in Figure 6.

https://doi.org/10.1021/acs.est.2c03962
Environ. Sci. Technol. 2022, 56, 16748−16758

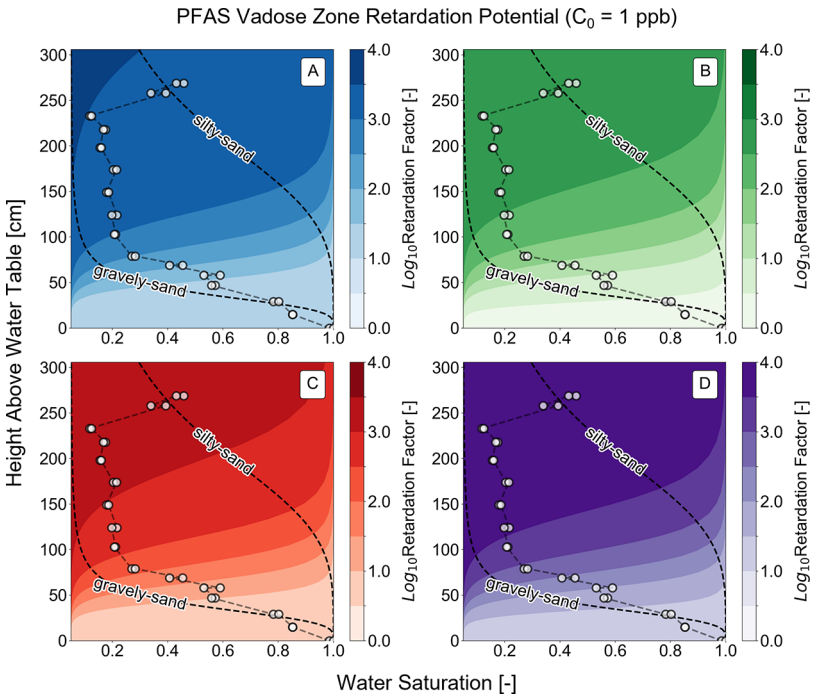

Figure 4. First-order approximations of the possible range of retardation experienced by PFOS (A), PFHxS (B), PFOA (C), and PFDA (D) in the vadose zone at a concentration of 1 [ppb]—derived from ultrapure water measurements. Two representative capillary pressure characteristic curves are shown, which constrain the site-wide heterogeneity. The measured capillary pressure profile of one sampled borehole (B006) is plotted to illustrate the effect of capillary heterogeneity on PFAA retardation. Log_{10} retardation factors are experienced throughout the vadose zone, suggesting nearly complete immobilization of PFAA.

Assuming a bulk-averaged organic carbon content (red lines in Figure 6), as opposed to the measured profile exhibiting spatial variability (blue lines in Figure 6), leads to overestimation of the vadose zone depth-averaged retardation of PFOS by approximately a factor of two. These results highlight that the identification of soil horizons containing a high content of organic carbon is key to accurate PFAA transport modeling.

Adsorption Model Selection. Adsorption model assumptions have a strong influence on the estimates of PFAA transport and retardation. For increasingly dilute PFAA solutions, K_{aw} will increase infinitely under a Freundlich adsorption model or reach a stable Γ_{max} when applying the Langmuir−Syszkowski model. Evidence may suggest that PFAA exhibits Freundlich adsorption at infinitely dilute concentrations and Langmuir−Syszkowski adsorption at higher concentrations.[29,43,58,75,76] Both Langmuir−Syszkowski and Freundlich models describe the data well; however, the mean ionic activity correction, C^*, did not adequately describe K_{aw} at elevated salt concentrations. By applying C^{*2}, or the square of mean ionic activity, we were able to describe the surface tension and K_{aw} well for concentrations below the CMC.[43,49] Further graphical comparisons between adsorption models and the effect on retardation can be found in Figure S3. Previous studies have proposed the use of a hybrid Langmuir−Freundlich adsorption model to more robustly describe air−water adsorption across high and low concentration ranges. Incorporating this model into the framework would likely improve the retardation estimates across concentration ranges.[53]

Freundlich isotherms have been widely shown to describe the solid-phase adsorption behavior of PFAA.[19,77,78] Our results indicate that the use of a linear K_d across narrower environmentally relevant concentrations in soils with minimal f_{oc} sufficiently describes the data. However, further experiments are required to determine if K_d can accurately be represented by additive mineral and organic carbon adsorption mechanisms.

Air−Water Interfacial Area Implications. In addition to adsorption model selection, the uncertainty surrounding the quantification of A_{wi} introduces significant complexity into the final retardation estimations. Several empirical and thermodynamic approaches have been developed with varying degrees of agreement.[21,22,32,39,46,47,79−81] Thermodynamic approaches have been shown to underestimate A_{wi}[81] and linear relationships fail to accurately represent the exponential increase of A_{wi} in heterogeneous geologic materials at low saturation.[79] The various approximations of A_{wi} can result in modeled mean breakthrough times ranging from years to decades.[81] Even experimental methods like interfacial tracer tests and X-ray micro-tomography can produce different A_{wi} measurements.[81,82]eq 10 was selected to link the van Genuchten model parameters measured at the field site to an approximate A_{wi} from the additional measured soil parameters. No measurements of A_{wi} were performed to validate the model on ORA soils. However, the model has demonstrated an ability to fit various soil types across narrow and wide particle size distributions.[46,47]

Long-Term PFAA Behavior. These results and analyses integrate the processes and conditions controlling PFAA sorption in the vadose zone into a framework for identifying and estimating long-term PFAA leaching to groundwater across a field site without the use of computationally intensive numerical models. As demonstrated, materials with low residual water saturation, typical of soils containing gravelly sand and thus high A_{wi}, will show elevated retardation factors compared to high residual soils, commonly silts and clays. A

https://doi.org/10.1021/acs.est.2c03962
Environ. Sci. Technol. 2022, 56, 16748−16758

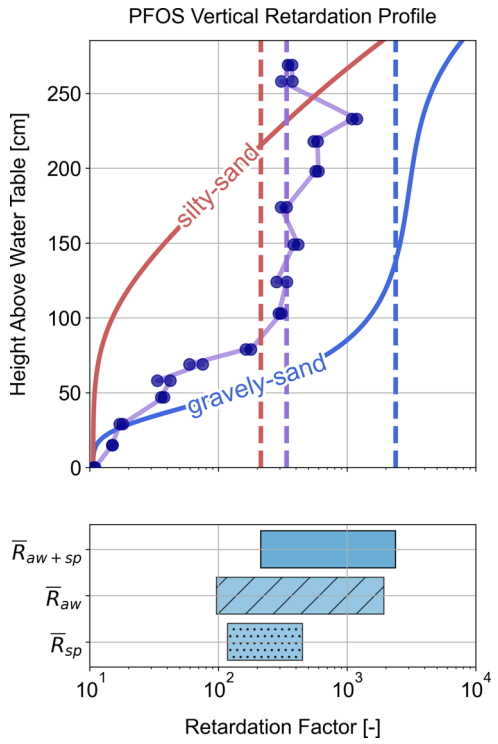

Figure 5. (Top) Application of the semi-analytical framework for PFOS at a concentration of 1 ppb. Depth-dependent retardation calculated based on ORA representative capillary pressure curves and borehole measurements (solid lines). The vertical dashed lines correspond to the vertically integrated retardation for each of these capillary pressure curves. (Bottom) Estimates of the upper bounds (corresponding to vertically integrated retardation in gravelly sand) and lower bounds (corresponding to vertically integrated retardation in silty sand) on PFOS retardation. Additional discrimination of air–water retardation ($\overline{R}_{aw}$) and solid-phase ($\overline{R}_{sp}$) retardation contributions is shown in relation to the combined retardation range ($\overline{R}_{aw+sp}$) in the lower bar plot. The upper and lower bounds are determined by the vertical integration of gravelly sand and silty sand, respectively.

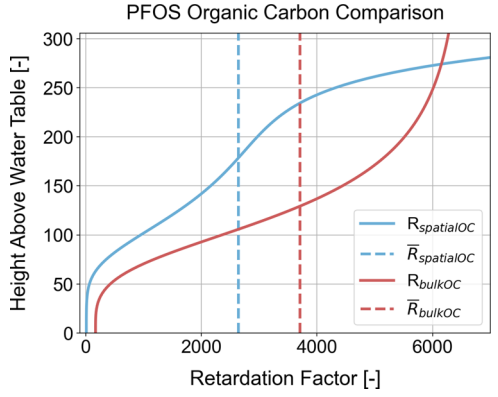

Figure 6. Comparison between a spatially distributed organic carbon profile ($R_{\text{spatial OC}}$) and a bulk-averaged organic carbon content of 1.7% ($R_{\text{bulk OC\%}}$) on PFOS retardation. The assumption of a bulk-averaged organic carbon content can increase the depth-averaged retardation values of PFAA, resulting in a longer than expected breakthrough.

large residual saturation will decrease the maximum A_{wi}, thus decreasing the overall retardation. This effect is due to the dominant influence of air–water adsorption on the overall PFAA retardation, as demonstrated in Figure 5.

This PFAA vadose zone retardation framework is based on hydrostatic capillary pressure conditions that do not vary in time. Under these stable water saturation conditions, PFAAs are likely to be nearly immobile in the vadose zone. However, the water saturation will temporarily increase during recharge events, such as high-intensity rain, flooding, or snowmelt. The result is a decrease in the retardation factor due to a reduction in the maximum A_{wi} and an increase in the saturation-dependent denominators of eq 1. After several wetting and drying periods, PFAA are expected to distribute throughout the vadose zone at lower concentrations, resulting in greater air–water interfacial retardation until Langmuir–Syszkowski adsorption stability is reached. Additional experimental work is needed to elucidate the coupled capillary pressure and PFAA remobilization behavior to account for transient water saturation conditions.

As a result of the static assumptions of this analysis, these results represent the upper and lower limits of retardation values throughout the vadose zone. The upper limit is represented by hydrostatic water saturation profiles and corresponding contributions due to air–water and solid-phase adsorption processes. Comparisons to previous modeling studies agree with the mechanisms and magnitude of the air–water-associated retardation in variably saturated media but do not yet account for possible air–water and solid-phase sorption heterogeneity.[23,27,33,83] The lower limit of retardation is represented by fully saturated conditions when solid-phase adsorption is the only mechanism contributing to PFAA retardation. As demonstrated, assumption of a bulk organic carbon content may result in a greater-than-expected retardation throughout the vadose zone profile—likely overestimating the PFAA travel time near the saturated boundary. Estimates of PFAA residence time in the vadose zone are loosely constrained by observations but are estimated to be on the order of decades.[6,8] While current transport models agree with decadal breakthrough timescales, observations of transient mobilization rates in unsaturated systems are necessary to constrain the PFAA travel time throughout the vadose zone.

■ ENVIRONMENTAL IMPLICATIONS

The emergent and ubiquitous nature of PFAS has created a critical need for the rapid and efficient determination of transport behavior at the field scale. The results of this study emphasize the influence of carbon chain length on the solid-phase and air–water adsorption mechanisms; both mechanisms drive increased sorption as the number of carbon chains increases. Additional influences, such as ionic strength and PFAA concentration, can further exaggerate the extent of retardation in the vadose zone. However, under unsaturated conditions, these results suggest that interfacial adsorption is largely responsible for the immobilization of PFAAs, explaining the observations of long-term adsorption and slow release of PFAAs to groundwater systems. Therefore, the vadose zone may act as a PFAA reservoir over long timescales.

The framework presented has demonstrated a need to validate several of the underlying models and approximations with experimental results. Future work is required to assess the adsorption behavior of PFAA and PFAA mixtures under heterogeneous unsaturated conditions. Additional experimental validation of air–water adsorption and interfacial area models will shed light on the impacts of PFAA adsorption in the presence of heterogeneity. Finally, sensitivity analyses will

https://doi.org/10.1021/acs.est.2c03962
Environ. Sci. Technol. 2022, 56, 16748–16758

help to discern the most important parameters to be built into future transport models.

The PFAA adsorption diagrams developed in this study (Figure 4) and vertical integration of collective retardation mechanisms (Figure 5) enable an estimate of PFAA retardation as a function of location in the vadose zone, PFAA concentration in the aqueous phase, solution chemistry, and geologic heterogeneity. This adaptive framework can be applied to broader categories of PFAS and PFAS mixtures, enabling mechanistic approximations of site location risk, PFAS sorption potential, and subsequent long-term leaching to groundwater without the use of numerical models. Vertical integration methods further enable the upscaling of complex heterogeneous PFAS retardation profiles. This depth-averaging approach can be used to parameterize transport models to more efficiently estimate and forecast field-scale PFAA fate and transport.

■ ASSOCIATED CONTENT

Supporting Information

The Supporting Information is available free of charge at https://pubs.acs.org/doi/10.1021/acs.est.2c03962.

PDF document containing five additional figures: adsorption model comparisons, solid-phase adsorption isotherms, air−water and solid phase adsorption profiles for saline and ultrapure solutions, and vadose zone retardation potentials for PFAAs in saline solution. The SI document includes two tables: air−water adsorption isotherm parameters and soil properties. Additional experimental details, materials, and methods are also provided (PDF)

■ AUTHOR INFORMATION

Corresponding Author

William R. Gnesda − *Department of Geoscience, University of Wisconsin—Madison, Madison, Wisconsin 53715, United States;* orcid.org/0000-0001-8968-2260; Email: gnesda@wisc.edu

Authors

Elliot F. Draxler − *Department of Civil and Environmental Engineering, University of Wisconsin—Madison, Madison, Wisconsin 53715, United States*

James Tinjum − *Department of Civil and Environmental Engineering, University of Wisconsin—Madison, Madison, Wisconsin 53715, United States*

Christopher Zahasky − *Department of Geoscience, University of Wisconsin—Madison, Madison, Wisconsin 53715, United States;* orcid.org/0000-0002-3427-5622

Complete contact information is available at: https://pubs.acs.org/10.1021/acs.est.2c03962

Notes

The authors declare no competing financial interest.

A Jupyter Notebook for figures 1-4 and 6 is available at https://doi.org/10.5281/zenodo.7319673.

■ ACKNOWLEDGMENTS

This material is based on work supported in part by the National Science Foundation under Grant Number EAR 2054263. Any opinions, findings, and conclusions or recommendations expressed in this material are those of the author(s) and do not necessarily reflect the views of the National Science Foundation. Additional support for this work was provided by the Office of the Vice Chancellor for Research and Graduate Education at the University of Wisconsin-Madison with funding from the Wisconsin Alumni Research Foundation and the Department of Geoscience Weeks Research Fellowship. The authors thank Sydney Klinzing, Nader A. Alhanaya, and Elizabeth Thomson for assistance with laboratory measurements.

■ REFERENCES

(1) Xiao, F.; Simcik, M. F.; Halbach, T. R.; Gulliver, J. S. Perfluorooctane sulfonate (PFOS) and perfluorooctanoate (PFOA) in soils and groundwater of a U.S. metropoli- tan area: Migration and implications for human exposure. *Water Res.* **2015**, *72*, 64−74.

(2) Sepulvado, J. G.; Blaine, A. C.; Hundal, L. S.; Higgins, C. P. Occurrence and fate of perfluorochemicals in soil following the land application of municipal biosolids. *Environ. Sci. Technol.* **2011**, *45*, 8106−8112.

(3) Guelfo, J. L.; Higgins, C. P. Subsurface transport potential of perfluoroalkyl acids at aqueous film-forming foam (AFFF)-impacted sites. *Environ. Sci. Technol.* **2013**, *47*, 4164−4171.

(4) Hoffman, K.; Webster, T. F.; Bartell, S. M.; Weisskopf, M. G.; Fletcher, T.; Vieira, V. M. Private drinking water wells as a source of exposure to perfluorooctanoic acid (PFOA) in communities surrounding a fluoropolymer production facility. *Environ. Health Perspect.* **2011**, *119*, 92−97.

(5) Shin, H. M.; Vieira, V. M.; Ryan, P. B.; Detwiler, R.; Sanders, B.; Steenland, K.; Bartell, S. M. Environmental fate and transport modeling for perfluorooctanoic acid emitted from the Washington works facility in West Virginia. *Environ. Sci. Technol.* **2011**, *45*, 1435−1442.

(6) Weber, A. K.; Barber, L. B.; Leblanc, D. R.; Sunderland, E. M.; Vecitis, C. D. Geochemical and Hydrologic Factors Controlling Subsurface Transport of Poly- and Perfluoroalkyl Substances, Cape Cod, Massachusetts. *Environ. Sci. Technol.* **2017**, *51*, 4269−4279.

(7) Röhler, K.; Haluska, A. A.; Susset, B.; Liu, B.; Grathwohl, P. Long-term behavior of PFAS in contaminated agricultural soils in Germany. *J. Contam. Hydrol.* **2021**, *241*, No. 103812.

(8) Høisæter, Å.; Pfaff, A.; Breedveld, G. D. Leaching and transport of PFAS from aqueous film-forming foam (AFFF) in the unsaturated soil at a firefighting training facility under cold climatic conditions. *J. Contam. Hydrol.* **2019**, *222*, 112−122.

(9) Zdziennicka, A.; Jańczuk, B. Behavior of anionic surfactants and short chain alcohols mixtures in the monolayer at the water-air interface. *J. Surfactants Deterg.* **2011**, *14*, 257−267.

(10) Brusseau, M. L. Assessing the potential contributions of additional retention processes to PFAS retardation in the subsurface. *Sci. Total Environ.* **2018**, *613-614*, 176−185.

(11) Interstate Technology & Regulatory Council (ITRC). *PFAS Technical and Regulatory Guidance Document and Fact Sheets PFAS*, 2021.

(12) Adamson, D. T.; Nickerson, A.; Kulkarni, P. R.; Higgins, C. P.; Popovic, J.; Field, J.; Rodowa, A.; Newell, C.; Deblanc, P.; Kornuc, J. J. Mass-Based, Field-Scale Demonstration of PFAS Retention within AFFF-Associated Source Areas. *Environ. Sci. Technol.* **2020**, *54*, 15768−15777.

(13) Xiao, F.; Jin, B.; Golovko, S. A.; Golovko, M. Y.; Xing, B. Sorption and Desorption Mechanisms of Cationic and Zwitterionic Per- And Polyfluoroalkyl Substances in Natural Soils: Thermodynamics and Hysteresis. *Environ. Sci. Technol.* **2019**, *53*, 11818−11827.

(14) Zhi, Y.; Liu, J. Sorption and desorption of anionic, cationic and zwitterionic polyfluoroalkyl substances by soil organic matter and pyrogenic carbonaceous materials. *Chem. Eng. J.* **2018**, *346*, 682−691.

(15) Li, Y.; Oliver, D. P.; Kookana, R. S. A critical analysis of published data to discern the role of soil and sediment properties in determining sorption of per and polyfluoroalkyl substances (PFASs). *Sci. Total Environ.* **2018**, *628−629*, 110−120.

(16) Higgins, C. P.; Luthy, R. G. Sorption of perfluorinated surfactants on sediments. *Environ. Sci. Technol.* **2006**, *40*, 7251−7256.
(17) Alves, A. V.; Tsianou, M.; Alexandridis, P. Fluorinated surfactant adsorption on mineral surfaces: implications for PFAS fate and transport in the environment. *Surfaces* **2020**, *3*, 516−566.
(18) Fabregat-Palau, J.; Vidal, M.; Rigol, A.Modelling the sorption behaviour of perfluoroalkyl carboxylates and perfluoroalkane sulfonates in soils. *Sci. Total Environ.***2021**, *801*. DOI: 10.1016/j.scitotenv.2021.149343.
(19) Li, F.; Fang, X.; Zhou, Z.; Liao, X.; Zou, J.; Yuan, B.; Sun, W. Adsorption of perfluorinated acids onto soils: Kinetics, isotherms, and influences of soil properties. *Sci. Total Environ.* **2019**, *649*, 504−514.
(20) Costanza, J.; Arshadi, M.; Abriola, L. M.; Pennell, K. D. Accumulation of PFOA and PFOS at the Air-Water Interface. *Environ. Sci. Technol. Lett.* **2019**, *6*, 487−491.
(21) Costanza-Robinson, M. S.; Brusseau, M. L. Air-water interfacial areas in unsaturated soils: Evaluation of interfacial domains. *Water Resour. Res.* **2002**, *38*, 13-1−13-17.
(22) Brusseau, M. L.; Yan, N.; van Glubt, S.; Wang, Y.; Chen, W.; Lyu, Y.; Dungan, B.; Carroll, K. C.; Holguin, F. O. Comprehensive retention model for PFAS transport in subsurface systems. *Water Res.* **2019**, *148*, 41−50.
(23) Guo, B.; Zeng, J.; Brusseau, M. L. A Mathematical Model for the Release, Transport, and Retention of Per- and Polyfluoroalkyl Substances (PFAS) in the Vadose Zone. *Water Resour. Res.* **2020**, *56*, No. e2019WR026667.
(24) van Glubt, S.; Brusseau, M. L. Contribution of nonaqueous-phase liquids to the retention and transport of per and polyfluoroalkyl substances (PFAs) in porous media. *Environ. Sci. Technol.* **2021**, *55*, 3706−3715.
(25) Silva, J. A.; Martin, W. A.; Johnson, J. L.; McCray, J. E. Evaluating air-water and NAPL-water interfacial adsorption and retention of Perfluorocarboxylic acids within the Vadose zone. *J. Contam. Hydrol.* **2019**, *223*, No. 103472.
(26) Lyu, Y.; Brusseau, M. L.; Chen, W.; Yan, N.; Fu, X.; Lin, X. Adsorption of PFOA at the Air-Water Interface during Transport in Unsaturated Porous Media. *Environ. Sci. Technol.* **2018**, *52*, 7745−7753.
(27) Brusseau, M. L.; Khan, N.; Wang, Y.; Yan, N.; van Glubt, S.; Carroll, K. C. Nonideal Transport and Extended Elution Tailing of PFOS in Soil. *Environ. Sci. Technol.* **2019**, *53*, 10654−10664.
(28) Brusseau, M. L. Simulating PFAS transport influenced by rate-limited multi-process retention. *Water Res.* **2020**, *168*, No. 115179.
(29) Stults, J. F.; Choi, Y. J.; Schaefer, C. E.; Illangasekare, T. H.; Higgins, C. P. Estimation of Transport Parameters of Perfluoroalkyl Acids (PFAAs) in Unsaturated Porous Media: Critical Experimental and Modeling Improvements. *Environ. Sci. Technol.* **2022**, *56*, 7963.
(30) Schaefer, C. E.; Culina, V.; Nguyen, D.; Field, J. Uptake of Poly- And Perfluoroalkyl Substances at the Air-Water Interface. *Environ. Sci. Technol.* **2019**, *53*, 12442−12448.
(31) Sharifan, H.; Bagheri, M.; Wang, D.; Burken, J. G.; Higgins, C. P.; Liang, Y.; Liu, J.; Schaefer, C. E.; Blotevogel, J. Fate and transport of per- and polyfluoroalkyl substances (PFASs) in the vadose zone. *Sci. Total Environ.* **2021**, *771*, No. 145427.
(32) Guo, B.; Zeng, J.; Brusseau, M. L.; Zhang, Y. A screening model for quantifying PFAS leaching in the vadose zone and mass discharge to groundwater. *Adv. Water Res.* **2022**, *160*, No. 104102.
(33) Silva, J. A. K.; Šimůnek, J.; McCray, J. E. A modified hydrus model for simulating pfas transport in the vadose zone. *Water* **2020**, *12*, No. 2758.
(34) Sima, M. W.; Jaffé, P. R. A critical review of modeling Poly- and Perfluoroalkyl Substances (PFAS) in the soil-water environment. *Sci. Total Environ.* **2021**, *757*, No. 143793.
(35) Barzegar, R.; Moghaddam, A. A.; Deo, R.; Fijani, E.; Tziritis, E. Mapping groundwater contamination risk of multiple aquifers using multi-model ensemble of machine learning algorithms. *Sci. Total Environ.* **2018**, *621*, 697−712.
(36) Sajedi-Hosseini, F.; Malekian, A.; Choubin, B.; Rahmati, O.; Cipullo, S.; Coulon, F.; Pradhan, B. A novel machine learning-based approach for the risk assessment of nitrate groundwater contamination. *Sci. Total Environ.* **2018**, *644*, 954−962.
(37) Singh, K. P.; Gupta, S.; Rai, P. Identifying pollution sources and predicting urban air quality using ensemble learning methods. *Atmos. Environ.* **2013**, *80*, 426−437.
(38) Brusseau, M. L.; Glubt, S. V. The influence of surfactant and solution composition on PFAS adsorption at fluid-fluid interfaces. *Water Res.* **2020**, *161*, 17−26.
(39) Kim, H.; Annable, M. D.; Rao, P. S. C. Influence of air-water interfacial adsorption and gas-phase partitioning on the transport of organic chemicals in unsaturated porous media. *Environ. Sci. Technol.* **1998**, *32*, 1253−1259.
(40) Brusseau, M. L.; Peng, S.; Schnaar, G.; Murao, A. Measuring air-water interfacial areas with X-ray microtomography and interfacial partitioning tracer tests. *Environ. Sci. Technol.* **2007**, *41*, 1956−1961.
(41) Balgooyen, S.; Remucal, C. K. Tributary Loading and Sediment Desorption as Sources of PFAS to Receiving Waters. *ACS EST Water* **2022**, *2*, 436−445.
(42) ASTM Standard D4646-16. Standard Test Method for 24-h Batch-Type Measurements of Contaminant Sorption by Soils and Sediments, ASTM International: West Conshohocken, PA, 2021, www.astm.org.
(43) Schaefer, C. E.; Drennan, D. M.; Tran, D. N.; Garcia, R.; Christie, E.; Higgins, C. P.; Field, J. A. Measurement of Aqueous Diffusivities for Perfluoroalkyl Acids. *J. Environ. Eng.* **2019**, *145*, No. 06019006.
(44) Langmuir, I. The constitution and fundamental properties of solids and liquids. II. liquids. *J. Am. Chem. Soc.* **1917**, *468*, 1848−1906.
(45) Freundlich, H. Kapillarchemie, Eine Darstellung der Chemie der Kolloide und verwandter Gebiete. *Nature* **1911**, *85*, 534−535.
(46) Peng, S.; Brusseau, M. L. Impact of soil texture on air-water interfacial areas in unsaturated sandy porous media. *Water Resour. Res.* **2005**, *41*, 1−8.
(47) Peng, S.; Brusseau, M. L. Air-water interfacial area and capillary pressure: porous-medium exture effects and an empirical function. *J. Hydrol. Eng.* **2012**, *17*, 829−832.
(48) Gurkov, T. D.; Dimitrova, D. T.; Marinova, K. G.; Bilke-Crause, C.; Gerber, C.; Ivanov, I. B. Ionic surfactants on fluid interfaces: Determination of the adsorption; Role of the salt and the type of the hydrophobic phase. *Colloids Surf., A* **2005**, *261*, 29−38.
(49) Wang, J.; Niven, R. K. Unification of surface tension isotherms of PFOA or GenX salts in electrolyte solutions by mean ionic activity. *Chemosphere* **2021**, *280*, No. 130715.
(50) Davies, C. The extent of dissociation of salts in water. Part VIII. An equation for the mean ionic activity coefficient of an electrolyte in water, and a revision of the dissociation constants of some sulphates. *J. Chem. Soc.* **1938**, 2093−2098.
(51) Robinson, R. A.; Stokes, R. H.*Electrolyte Solutions*; Courier Corporation, 2002.
(52) Lunkenheimer, K.; Prescher, D.; Hirte, R.; Geggel, K. Adsorption properties of surface chemically pure sodium perfluoro-N -alkanoates at the Air/water interface: Counterion effects within homologous series of 1:1 ionic surfactants. *Langmuir* **2015**, *31*, 970−981.
(53) Silva, J. A.; Martin, W. A.; McCray, J. E. Air-water interfacial adsorption coefficients for PFAS when present as a multi-component mixture. *J. Contam. Hydrol.* **2021**, *236*, No. 103731.
(54) Huang, D.; Saleem, H.; Guo, B.; Brusseau, M. L. The impact of multiple-component PFAS solutions on fluid-fluid interfacial adsorption and transport of PFOS in unsaturated porous media. *Sci. Total Environ.* **2022**, *806*, No. 150595.
(55) Houtz, E. F.; Higgins, C. P.; Field, J. A.; Sedlak, D. L. Persistence of perfluoroalkyl acid precursors in AFFF-impacted groundwater and soil. *Environ. Sci. Technol.* **2013**, *47*, 8187−8195.
(56) Ruyle, B. J.; Thackray, C. P.; McCord, J. P.; Strynar, M. J.; Mauge-Lewis, K. A.; Fenton, S. E.; Sunderland, E. M. Reconstructing the Composition of Per- And Polyfluoroalkyl Substances in

Contemporary Aqueous Film-Forming Foams. *Environ. Sci. Technol. Lett.* **2021**, *8*, 59−65.
(57) Vecitis, C. D.; Park, H.; Cheng, J.; Mader, B. T.; Hoffmann, M. R. Enhancement of perfluorooctanoate and perfluorooctanesulfonate activity at acoustic cavitation bubble interfaces. *J. Phys. Chem. C* **2008**, *112*, 16850−16857.
(58) Arshadi, M.; Costanza, J.; Abriola, L. M.; Pennell, K. D. Comment on "uptake of Poly- And Perfluoroalkyl Substances at the Air-Water Interface. *Environ. Sci. Technol.* **2020**, *54*, 7019−7020.
(59) Wang, Z.; Dewitt, J. C.; Higgins, C. P.; Cousins, I. T. A Never-Ending Story of Per- and Polyfluoroalkyl Substances (PFASs)? *Environ. Sci. Technol.* **2017**, *51*, 2508−2518.
(60) van Genuchten, M. T. A Closed-form Equation for Predicting the Hydraulic Conductivity of Unsaturated Soils. *Soil Sci. Soc. Am. J.* **1980**, *44*, 892−898.
(61) Bardestani, R.; Patience, G. S.; Kaliaguine, S. Experimental methods in chemical engineering: specific surface area and pore size distribution measurements−BET, BJH, and DFT. *Can. J. Chem. Eng.* **2019**, *97*, 2781−2791.
(62) Valocchi, A. J. Spatial moment analysis of the transport of kinetically adsorbing solutes through stratified aquifers. *Water Resour. Res.* **1989**, *25*, 273−279.
(63) Krall, K.*PFAS Found In Rhinelander Well, Drinking Water Safe, Crescent Spring To Be Tested*, 2019.
(64) Attig, J. W.; Rawling, J. E. In *Influence of Persistent Buried Ice on Late Glacial Landscape Development in Part of Wisconsinas Northern Highlands*, Special Paper of The Geological Society of America, 2018; pp 103−114.
(65) Aslesen, A.*City of Rhinelander Wellhead Protection Plan*, 2015.
(66) Lv, X.; Sun, Y.; Ji, R.; Gao, B.; Wu, J.; Lu, Q.; Jiang, H. Physicochemical factors controlling the retention and transport of perfluorooctanoic acid (PFOA) in saturated sand and limestone porous media. *Water Res.* **2018**, *141*, 251−258.
(67) Kissa, E.*Fluorinated Surfactants and Repellents*; CRC Press, 2001; Vol. *97*.
(68) Meissner, H.; Michaels, A. Surface tensions of pure liquids and mixtures. *Ind. Eng. Chem.* **1949**, *41*, 2782−2787.
(69) Wang, J. P.; Lambert, P.; de Kock, T.; Cnudde, V.; François, B. Investigation of the effect of specific interfacial area on strength of unsaturated granular materials by X-ray tomography. *Acta Geotech.* **2019**, *14*, 1545−1559.
(70) Brooks, R. H.; Corey, A. Properties of Porous Media Affecting Fluid Flow. *J. Irrig. Drain. Div.* **1966**, *92*, 61−88.
(71) Poulsen, M. M.; Kueper, B. H. A Field Experiment to Study the Behavior of Tetrachloroethylene in Unsaturated Porous Media. *Environ. Sci. Technol.* **1992**, *26*, 889−895.
(72) Leverett, M. In *Capillary Behavior in Porous Solids*, Transactions of the AIME, 1940; pp 152−169.
(73) Pini, R.; Benson, S. M. Characterization and scaling of mesoscale heterogeneities in sandstones. *Geophys. Res. Lett.* **2013**, *40*, 3903−3908.
(74) Zahasky, C.; Jackson, S. J.; Lin, Q.; Krevor, S. Pore Network Model Predictions of Darcy-Scale Multiphase Flow Heterogeneity Validated by Experiments. *Water Resour. Res.* **2020**, *56*, No. e2019WR026708.
(75) Fainerman, V.; Lucassen-Reynders, E. Adsorption of single and mixed ionic surfactants at fluid interfaces. *Adv. Colloid Interface Sci.* **2002**, *96*, 295−323.
(76) Guelfo, J. L.; Adamson, D. T. Evaluation of a national data set for insights into sources, composition, and concentrations of per-and polyfluoroalkyl substances (PFASs) in US drinking water. *Environ. Pollut.* **2018**, *236*, 505−513.
(77) Milinovic, J.; Lacorte, S.; Vidal, M.; Rigol, A. Sorption behaviour of perfluoroalkyl substances in soils. *Sci. Total Environ.* **2015**, *511*, 63−71.
(78) Mejia-Avendaño, S.; Zhi, Y.; Yan, B.; Liu, J. Sorption of Polyfluoroalkyl Surfactants on Surface Soils: Effect of Molecular Structures, Soil Properties, and Solution Chemistry. *Environ. Sci. Technol.* **2020**, *54*, 1513−1521.
(79) Schaefer, C. E.; DiCarlo, D. A.; Blunt, M. J. Experimental measurement of air-water interfacial area during gravity drainage and secondary imbibition in porous media. *Water Resour. Res.* **2000**, *36*, 885−890.
(80) Silva, J. A.; Šimůnek, J.; McCray, J. E. Comparison of methods to estimate air-water interfacial areas for evaluating PFAS transport in the vadose zone. *J. Contam. Hydrol.* **2022**, *247*, No. 103984.
(81) Brusseau, M. L.; Guo, B. Air-water interfacial areas relevant for transport of per and poly-fluoroalkyl substances. *Water Res.* **2021**, *207*, No. 117785.
(82) Brusseau, M. L.; Peng, S.; Schnaar, G.; Costanza-Robinson, M. S. Relationships among air-water interfacial area, capillary pressure, and water saturation for a sandy porous medium. *Water Resour. Res.* **2006**, *42*, No. W03501.
(83) Brusseau, M. L.; Anderson, R. H.; Guo, B. PFAS concentrations in soils: Background levels versus contaminated sites. *Sci. Total Environ.* **2020**, *740*, No. 140017.

https://doi.org/10.1021/acs.est.2c03962
Environ. Sci. Technol. 2022, 56, 16748−16758